Shahid Chamran University of Ahvaz

Iranian Association of Electrical and Electronics Engineers

Journal of Applied Research in Electrical Engineering

E-ISSN: 2783-2864
P-ISSN: 2717-414X
Homepage: https://jaree.scu.ac.ir/

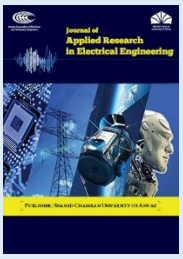

Research Article

Designing of the Controller for Shipboard Microgrid Based on Linear Matrix Inequality

Farhad Amiri, Mohammad Hassan Moradi*

Electrical Engineering Department, Faculty of Engineering, Bu-Ali Sina University, Hamedan 6516738695, Iran

** Corresponding Author: mh_moradi@yahoo.co.uk*

Abstract: With the presence of distributed energy resources in microgrids, the problem of load-frequency control (LFC) becomes one of the most important concerns. Changes in the parameters of the microgrid components, as well as the disturbances forced on the grid, make it more difficult to design a suitable LFC. This paper discusses the design of a robust model predictive controller (RMPC) based on the linear matrix inequality as a secondary controller in LFC systems for controlling a microgrid on the shipboard. The main purpose of the proposed method is to improve the frequency stability of the microgrid in the presence of disturbances and the uncertainty of its parameters. The proposed controller is simulated and compared in several different scenarios considering the uncertainty of the microgrid parameters and the input disturbances. The main controllers are the fuzzy proportional-integral type 1 and 2, and multi-objective multi-purpose functions optimized with the MOFPI (MBBHA) and MOIT2FPI (MBHA) algorithms. The effectiveness of the proposed method in terms of increasing the response speed, reducing fluctuations, overcoming uncertainties of the parameters, and ensuring robustness to disturbances are discussed. The simulations are made in MATLAB software. The proposed method reduces the frequency oscillations caused by disturbances on the microgrid by 68% (68% improvement over other methods used in this field). Also, using this method, the damping speed of microgrid frequency fluctuations is increased by 53% (performance improvement).

Keywords: Microgrid on the shipboard, load-frequency control, linear matrix inequality, uncertainty.

Article history
Received 17 December 2021; Revised 27 February 2022; Accepted 02 March 2022; Published online 17 March 2022.

How to cite this article
F. Amiri, and M. H. Moradi, "Designing of the controller for shipboard microgrid based on linear matrix inequality," *J. Appl. Res. Electr. Eng.*, vol. 1, no. 2, pp. 175-185, 2022. DOI: 10.22055/jaree.2022.39484.1041

Check for updates

1. INTRODUCTION

The increasing need for electrical power has forced system operators to use more renewable energy resources. However, despite their many advantages in comparison with fossil-based resources, the energy resources increase the control complexity and pose many challenges to system stability and security [1, 2]. Renewable energy resources are often used as an alternative resource in modern power systems. Although increasing the penetration of these energy resources has many advantages, it poses new challenges, e.g., whether these resources can be operated beside the existing generation units properly [1, 2]. Two of the major challenges in distributed generation resources and energy storage resources are the regulation of the system voltage and frequency and if it is a suitable and proper control design both in network-connected and isolated mode.

The concept of the microgrid, which is a combination of renewable energy resources, storage devices, communication systems, loads, and controllers, was introduced in 1998. Microgrids are usually located on the distribution side and can be connected to or isolated from the upstream network. In a network-connected microgrid, it is responsible to inject real and reactive power into the system, while in the isolated mode, it is responsible for providing local loads and adjusting frequency and voltage characteristics in the nominal value. As a result, the role of automatic control is more fundamental in microgrids due to more generation and load disturbances. In the steady-state, microgrids are in equilibrium between production and consumption. If this equilibrium is lost, the frequency will deviate from its nominal value. If frequency deviations are not controlled, they can cause a lot of damage [1]. Frequency variations are very important in microgrids and

must always be in an acceptable bond. For example, if the load increases suddenly, the frequency will drop from the nominal value, which will lead to frequency instability if not controlled.

The primary-control loop is the first control loop that reacts to limit the frequency drop after unwanted events [2]. The primary-control loop limits the dropped frequency, but it is unable to return the frequency to its nominal value, and thus another control loop, called the frequency secondary control, is used [2]. The secondary-control loop is controlled by the load-frequency control (LFC). Different controllers are used in the second control loop. Due to the random and uncertain nature of wind, solar radiation, and sea waves, the power derived from renewable energy resources varies randomly. Random variations of generated power and load variations can cause load-generation imbalance and significant deviations in the microgrid frequency, especially in the isolated mode [2]. Among many factors that are important in the design of LFC, one of the most important challenges is the uncertainty in the parameters of the microgrid components. LFC approaches have already been used in research studies to eliminate the generation and frequency variations, return the frequency to the nominal value, and restore the power of the transmission line [2, 3]. Some researchers have specifically concentrated on microgrids [4-27].

Several controllers, such as typical PI [4-6], typical PID, PID based on the Ziggler-Nichols coefficient method [7], PID based on the genetic algorithm [8], PI based on PSO [9], biogeography-based PID [10], PI/PID based on quasi-oppositional harmony search algorithm (QOH) [11], fractional-order PID [12], fuzzy-PID based on fractional-order [13], PI based on fuzzy logic type 2 in combination with improved harmony search algorithm [14, 15], have been introduced for controlling load-frequency in microgrids. Also, H infinite control ($H\infty$) methods [16-18], fuzzy-based pso control [19], and human brain emotional learning (HBEL) [20] are some other approaches to controlling load-frequency in microgrids. In [21], the time delay effect of telecommunication systems on the load-frequency control in a multi-region system is investigated. In [22], the tertiary monitoring control strategy for controlling load-frequency in a multi-region microgrid system is introduced. In [23], fuzzy PID-based control is presented in a small three-zone system for LFC. In [24], the effect of transmission lines and super-capacitors on load-frequency control in a multi-region network is investigated. In [25], the effect of storage systems on LFC in a multi-region network is discussed. In [26], the load-frequency control is presented in a multi-region microgrid with the fuzzy PID control adjusted by the Nagai method. In [27], the load-frequency control is presented in a two-zone microgrid network with PID based on a social-spider optimizer (SSO). In [28], the load-frequency control of an isolated microgrid is investigated on the ship by a type-I and multi-objective fuzzy proportional controller, which is optimized with the online black hole algorithm.

In the proposed methods [4-27], the problem of uncertainty of system parameters (microgrid) has not been addressed for the load-frequency control loop of microgrids. The uncertainty of microgrid parameters jeopardizes the performance of the load frequency control loop and may cause microgrid frequency instability. On the other hand, severe load disturbances and distributed energy resources are effective in the performance of this loop. When faced with severe disturbances, the loop may not be able to function properly, and the microgrid may experience frequency instability. Therefore, in the load-frequency control structure, it is necessary to have a robust controller that can attenuate disturbances on the islanded microgrid and is resistant to the uncertainty of the parameters in order to ensure the frequency stability of the microgrid.

This paper presents a control method (robust model predictive controller) for the load-frequency control loop. The robust model predictive controller is based on linear matrix inequality, and the proof of this method is based on the Lyapunov stability criterion. The proposed method can attenuate the disturbances on the microgrid on the shipboard and is very resistant to the uncertainty of the microgrid parameters. In other words, the proposed method is capable of maintaining the frequency stability of the microgrid under disturbance and parametric uncertainty. To prove the efficiency of the proposed method, several scenarios have been considered and compared with several methods used in this field.

The rest of this paper is organized as follows. Section 2 introduces the components and model of a microgrid on the slope of the shipboard. Section 3 introduces the proposed control method for microgrids based on linear matrix inequality. In Section 4, simulations are performed in several scenarios to prove the improvement of microgrid performance using the proposed controller. Finally, the conclusion is given in Section 5.

2. Components and Model of a Microgrid on the Shipboard

2.1. The Model of Microgrid on the Shipboard

A microgrid on the shipboard based on LFC is depicted in Fig. 1. Microgrids on shipboards consist of photovoltaic (PV), a wind turbine (WT), a sea wave energy converter, a diesel generator (DG), a flywheel energy storage system (FESS), and a battery energy storage system (BESS). The photovoltaic, wind turbine, and wave energy converters are the main sources of load supply, but due to their power variations, the diesel generator acts as a backup power source to respond to load variations. BESS and FESS consume the surplus power and compensate for the load in the short term [23-28]. The dynamical model of each microgrid resource on the shipboard is discussed below. A microgrid on the ship is depicted in Fig 2, which represents an islanded microgrid on the ship, which includes energy resources such as wind turbines, photovoltaic, sea wave energy converters, diesel generators, and energy storage devices such as batteries and flywheels.

2.2. Wind Turbine (WT):

The wind turbine is a component that is used to convert wind energy into mechanical and electrical energy. The wind turbine power (P_{WT}) is calculated by (1) [7-9]. The dynamic model of the wind turbine is considered the first-order transform function, which is defined as (2).

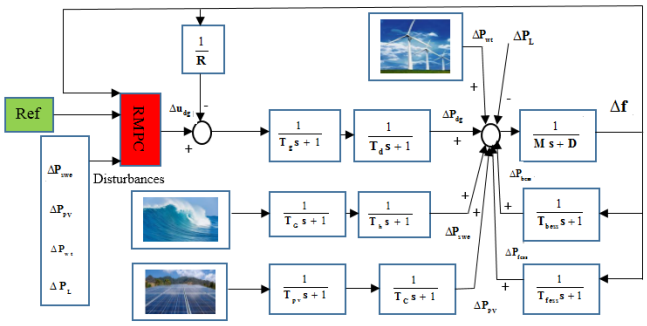

Fig. 1: A schematic of microgrids on shipboards based on the LFC.

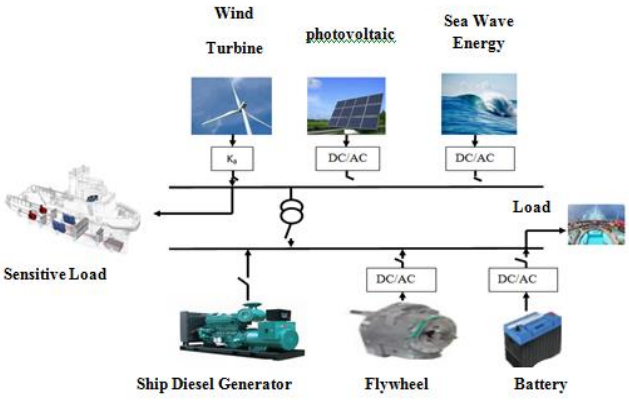

Fig. 2: A schematic of microgrids on shipboards.

$$P_{WT} = \frac{1}{2} C_{\rho}(\beta, \lambda) \rho A V_w^3 \quad (1)$$

$$G_{WT} = \frac{k_{WT}}{T_{WT} s + 1} \quad (2)$$

In (1), ρ is the air density, A is the surface swept by the blades, V_w is the wind speed, and $C_{\rho}(\beta, \lambda)$ is the turbine performance factor that depends on the environmental conditions and how the turbine is made. In (2), T_{WT}, k_{WT} are the wind turbine gain and time constant, respectively [7, 9].

2.3. Photovoltaic (Solar Cell)

The photovoltaic converts solar energy into electrical energy [4-5]. Solar power is dependent on temperature and radiation. The dynamical model of the solar cell with the inverter model is represented by (3) and (4) [4-5]. The inverter and photovoltaic model are considered a first-order transform function. In (3), *Tc* is the time constant of the inverter related to the photovoltaic, and in (4), and *Tpv* is the time constant of the photovoltaic.

$$G_c = \frac{1}{T_c s + 1} \quad (3)$$

$$G_{pv} = \frac{1}{T_{pv} + 1} \quad (4)$$

2.4. Sea Wave Energy (SWE)

The energy of sea waves is considered a distributed energy resource. The conversion of sea waves into energy is carried out by wave energy converter (WEC). In this study, the energy of sea waves is considered a renewable energy resource. Also, the transform function of the wave converter for shipboards is considered a first-order time delay [28].

2.5. Diesel Generator Model (DG)

The block diagram of a diesel generator and governor is shown in Fig. 3, which includes the droop control loop R. A first-order time delay for the valve drive system and diesel engine with the time constants Tg and Td are shown, respectively. Δu_{dg} is the load-frequency control signal and ΔF is the frequency deviation. ΔX_g is the valve position [6].

2.6. Battery Energy Storage Model (BESS)

The battery stores electrical energy in the form of chemical mechanism and DC voltage. It requires a charger and an inverter to generate AC current and voltages. In this paper, an oxidation battery is used due to its features, including higher capacity, quicker mechanism, and discharge during the operation. The battery model and the inverter connected to the microgrid are represented as a first-order time delay in (5). T_{bess} is the battery time constant [12].

$$\frac{1}{T_{bess} s + 1} \quad (5)$$

2.7. Flywheel Energy Storage System (FESS)

In the flywheel, the energy is stored as kinetic energy. Equation (6) represents the kinetic energy [12, 28]. In (6), I is the inertia of the flywheel and *W* is the angular velocity (rad/sec). The dynamic model of the flywheel is represented as the first-order transform function in (7). T_{fess} is the time constant of the flywheel [12, 28].

$$k_E = \frac{1}{2} I W^2 \quad (6)$$

$$G_{fess} = \frac{1}{T_{fess} s + 1} \quad (7)$$

2.8. Model of the Rotoring Mass on the Shipboard

To keep the microgrid on the shipboard in a stable and balanced situation, frequency deviation occurs with power changes. In practice, however, there is a time delay between the system power deviation and frequency deviation. The rotor-mass model of microgrids on shipboards is shown in (8). In (8), *M* is the inertia constant and *D* is the damping constant [7, 28]

$$G = \frac{1}{Ms + D} \quad (8)$$

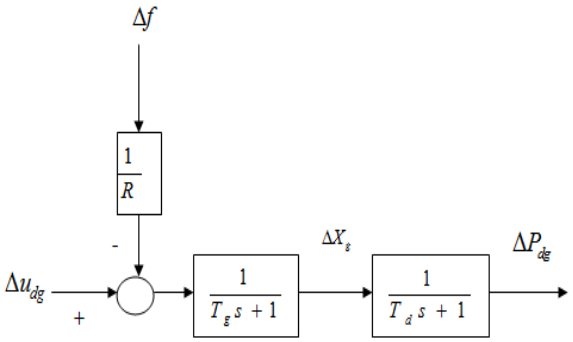

Fig. 3: The dynamic model of diesel generators.

2.9. The Load Dynamic Model

This paper presents two different types of shiploads, which are equivalent to asynchronous motors and the resistive load with respect to 350 HP and 400 kW, separately. The variations of the shiploads are also considered. The variations of the shipload in this paper only include the variations of the resistive loads. The dynamic model of the variations of the resistive loads is shown in Fig. 4. The standard deviation is multiplied by the random output fluctuations derived from the white noise block in MATLAB/SIMULINK to simulate the real-time random power fluctuations on the load profile [28, 29].

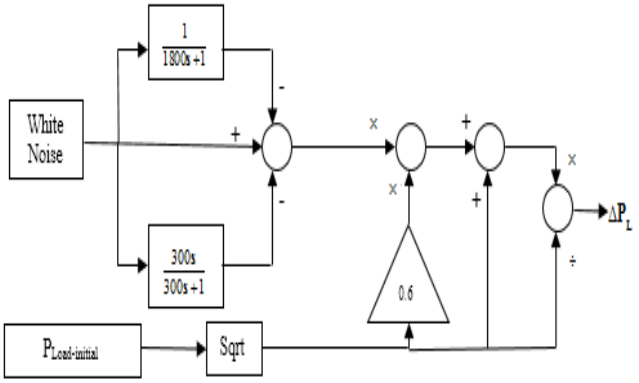

Fig. 4: The dynamic model of the variations of the resistive loads

3. Designing a Proposed Control Method for Microgrid based on Linear Matrix Inequality

3.1. Dynamic Model of Microgrid on the Shipboard

First, according to Fig. 1, linear equations at the operating point of the microgrid on the ship are introduced as (9)-(13).

$$\Delta \dot{X}_g = \frac{\Delta u_{dg}}{T_g} - \frac{\Delta f}{RT_g} - \frac{\Delta X_g}{T_g} \tag{9}$$

$$\Delta \dot{P}_{dg} = \frac{\Delta X_g}{T_d} - \frac{\Delta P_{dg}}{T_d} \tag{10}$$

$$\Delta \dot{P}_{fess} = \frac{\Delta f}{T_{fess}} - \frac{\Delta P_{fess}}{T_{fess}} \tag{11}$$

$$\Delta \dot{P}_{bess} = \frac{\Delta f}{T_{bess}} - \frac{\Delta P_{bess}}{T_{bess}} \tag{12}$$

$$\Delta \dot{f} = \frac{-D \times \Delta f}{M} - \frac{\Delta P_L}{M} + \frac{\Delta P_{swe}}{M} + \frac{\Delta P_{bess}}{M} + \frac{\Delta P_{pv}}{M} + \frac{\Delta P_{wt}}{M} + \frac{\Delta P_{dg}}{M} + \frac{\Delta P_{fess}}{M} \tag{13}$$

In (9)-(13), ΔP_{fess} is the flywheel power, ΔP_{bess} is the battery power, ΔP_L is the Load variation, ΔP_{swe} is the power taken from sea waves, ΔP_{PV} is the photovoltaic power, ΔP_{wt} is the wind turbine power, R is the dropped factor, Δu_{dg} is the signal sent to the generator, ΔX_g is the output generator changes, and ΔP_{dg} is the diesel generator changes. The state equations are represented as (14). Based on (14), the equations of the microgrid states on the ship are obtained as (15) and (16).

$$\begin{aligned} \dot{X} &= AX + BU + DW \\ Y &= CX \end{aligned} \tag{14}$$

in which X is the vector of state variables for the model predictive control, A is the model predictive control state space, matrix U is the model predictive control output vector, B is the model predictive control coefficients matrix, W is the disturbance vector (uncontrolled input) of model predictive control, and D is the disturbance coefficient matrix.

$$\begin{bmatrix} \Delta \dot{X}_g \\ \Delta \dot{P}_{dg} \\ \Delta \dot{P}_{fess} \\ \Delta \dot{P}_{bess} \\ \Delta \dot{f} \end{bmatrix} = \begin{bmatrix} \frac{-1}{T_g} & 0 & 0 & 0 & -\frac{1}{R \times T_g} \\ \frac{1}{T_d} & \frac{-1}{T_d} & 0 & 0 & 0 \\ 0 & 0 & \frac{-1}{T_{fess}} & 0 & \frac{1}{T_{fess}} \\ 0 & 0 & 0 & \frac{-1}{T_{bess}} & \frac{1}{T_{bess}} \\ 0 & \frac{1}{M} & \frac{1}{M} & \frac{1}{M} & \frac{-D}{M} \end{bmatrix} \begin{bmatrix} \Delta X_g \\ \Delta P_{dg} \\ \Delta P_{fess} \\ \Delta P_{bess} \\ \Delta f \end{bmatrix} + \begin{bmatrix} \frac{1}{T_g} \\ 0 \\ 0 \\ 0 \\ 0 \end{bmatrix} \left[\Delta u_{dg} \right] + \begin{bmatrix} 0 \\ 0 \\ 0 \\ 0 \\ \frac{1}{M} \end{bmatrix} \left[\Delta P_{wt} + \Delta P_{swe} + \Delta P_{pv} - \Delta P_L \right] \tag{15}$$

$$y=\begin{bmatrix}0 & 0 & 0 & 0 & 1\end{bmatrix}\begin{bmatrix}\Delta X_g\\ \Delta P_{dg}\\ \Delta P_{fess}\\ \Delta P_{bess}\\ \Delta f\end{bmatrix} \quad (16)$$

3.2. Model Predictive Control (MPC)

In the model predictive control, the control signal is obtained by minimizing a cost function. The control signal values in the control horizon are determined so that the system outputs follow the specified reference path in the future and on a given horizon. For this purpose, the cost function, which is generally considered the square of the deviation of the controlled variables from the desired values, is minimized [29-35]. The structure of the model predictive control is depicted in Fig. 5.

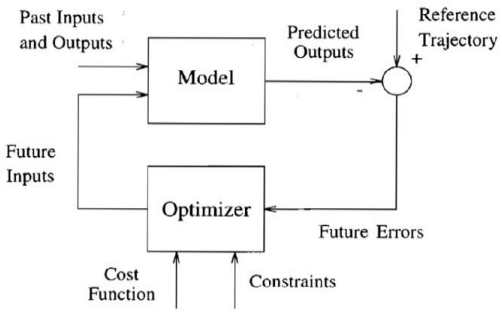

Fig. 5: The structure of the model predictive control.

3.3. Converting the Model Predictive Control to the Robust Model Predictive Control

Firstly, the state space of a microgrid on the shipboard obtained from (15) and (16) is introduced in the discrete form as (17). The objective function of the model predictive control is defined as (18). In (18), J(k) is the cost function at time k, N_2 is the upper prediction horizon, Q_1 is the weighting coefficient, R is the weight factor, and u (k + i) is the control signal.

First, uncertainty is introduced in the prediction model control for which multi-dimensional uncertainty is implemented as (19). $A(k), B(k)$ are the dynamical time-varying matrices. In a convex set Ω, there are all possibilities for $A(k), B(k)$ which is expressed in (20). As a result, the objective function of the model predictive control is expressed as (21). The purpose of the robust model predictive control problem is to find the coefficient *F* in (22) in such a way that on a certain horizon, a huge number of cost functions in (21) is minimized. By obtaining a control signal *F* and implementing it in the process, the output is re-measured and the optimization problem is solved again. To apply the minimization problem to the maximization of uncertainty problems, an upper bound is defined in (18) as the Lyapunov function (23). The Lyapunov function is defined as in (24). Given (23) and (24), if a matrix P is found in such a way that it is greater than the cost function, for all situations the uncertainty is taken into account in the matrix *P*. The stability condition of the Lyapunov function is $V(k+1)-V(k)<0$ and P>0. Considering (25), if the left-hand side of (25) is summed up from j–and from the left $-V(x(k))$, it will be $i=0\to\infty$ from the right. Finally, it leads to (26), and eventually, the upper bound of the cost function is found. Therefore, (26) is transformed into a squared Lyapunov function and implicitly implies the uncertainties of the system. (27) is obtained by defining an upper bound for (26). The modified (28) of (27) has the constraints to solve the robust prediction control problem.

To solve the problem, the constraint in (28) is represented as (29) using linear matrix inequality and Schur complement. The stability condition of the Lyapunov function is also introduced as (30) in which L is the number of vertices in the multi-dimensional model. The constraints on the input of the system are formed as (31) that is transformed into (32) using matrix inequalities. The constraints on the output of the system are formed as (33) that is transformed into (34) using matrix inequalities.

$$x(k+1)=Ax(k)+Bu(k)$$
$$y(k)=Cx(k) \quad (17)$$

$$\min_{u(k+i),i=1,2,...,N_2} j(k) \quad (18)$$
$$j(k)=\sum_{0}^{N_2}(x(k+i)^T Q_1 x(k+i)+u(k+i)^T Ru(k+i))$$

$$\left[A(k)\ B(k)\right]\in\Omega \quad (19)$$

$$\Omega=Co\{[A_1,B_1],[A_2,B_2],...,[A_L,B_L]\} \quad (20)$$

$$\min_{u(k+i),i=1,2,...,N_2}\ \max_{[A(k+i),B(k+i)]\in\Omega} j_\infty(k) \quad (21)$$

$$u(k+i)=Fx(k+i) \quad (22)$$

$$j_\infty<V(x(k)) \quad (23)$$

$$V(x(k))=x^T(k)Px(k) \quad (24)$$

$$V(x(k+i+1|k))-V(x(k+i|k))<$$
$$-(x(k+i|k)^T Q_1 x(k+i|k)+u(k+i|k)^T Ru(k+i|k)) \quad (25)$$

$$\min_{u(k+i),i=1,...,N_2} V(x(k)) \quad (26)$$

$$\min_{x^T(k)Px(k)\le\eta}\ \eta \quad (27)$$

$$\min_{\gamma,Q,Y}\ \gamma \quad (28)$$

$$\begin{bmatrix} 1 & x^T(k) \\ x(k) & Q \end{bmatrix} \geq 0 \tag{29}$$

$$\begin{bmatrix} Q & QA_j^T + Y^T B_j^T & QQ_1^{\frac{1}{2}} & Y^T R^{\frac{1}{2}} \\ A_j Q + B_j Y & Q & 0 & 0 \\ Q_1^{\frac{1}{2}} Q & 0 & \eta I & 0 \\ R^{\frac{1}{2}} Y & 0 & 0 & \eta I \end{bmatrix} \geq 0 \quad j = 1,2,...,L \tag{30}$$

$$\left\| u(k+i|k) \right\|_2 \leq u_{\max} \tag{31}$$

$$\begin{bmatrix} u_{\max}^2 I & Y \\ Y^T & Q \end{bmatrix} \geq 0 \tag{32}$$

$$\left\| y(k+i|k) \right\|_2 \leq y_{\max} \tag{33}$$

$$\begin{bmatrix} Q & (A_j Q + B_j Y)^T C^T \\ C(A_j Q + B_j Y)^T C^T & Q \end{bmatrix} \geq 0 \quad j = 1,2,...,L \tag{34}$$

3.4. Designing a Robust Model Predictive Control System for the Problem

1) Form the continuous state-space system

2) Convert the continuous state space to a discrete state space using the Euler approximation method

3) Minimize (28) by considering the constraints (29), (30), (32), and (34).

4) Calculate the control signal and apply it to the system

The flowchart of the method proposed for solving the problem is shown in Fig. 6. The proof of the above equations is given in [31-36].

4. SIMULATION

4.1. Parameters Related to the Microgrid on the Shipboard

The parameters of a microgrid on the ship are provided in Table 1.

4.2. Scenarios

In the first scenario, the load disturbances in a microgrid are considered without any regard to the power generated from distributed energy resources. In the second scenario, disturbances of the distributed energy resources are considered and finally, in the third scenario, load disturbances with given uncertainty of the parameters are considered.

Scenario (1): In this scenario, the changes in the distributed energy resources are not considered, and only load disturbances are considered. The load disturbances have been applied to the microgrid according to Fig. 7. In Fig. 8, the frequency response of the microgrid is in terms of load disturbances. The maximum frequency deviation using the proposed method is 0.005 Hz. The maximum frequency deviation using a multi-objective fuzzy proportional-integral controller type 2 optimized by the black hole algorithm is 0.027 Hz. The maximum frequency deviation using a multi-objective proportional-integral controller optimized with the black hole algorithm is 0.033 Hz. As can be seen in the simulation results, the proposed RMPC in comparison with the multi-objective proportional-integral controller optimized with the black hole algorithm [28] and multi-objective fuzzy proportional-integral controller type 2 optimized by the black hole algorithm [28] has a better response speed and lower fluctuation and is more robust to load disturbances.

Scenario (2): In this scenario, changes in distributed energy resources are considered while load disturbances aren't. Disturbances of distributed energy resources (wind turbine, photovoltaic, sea wave) have been applied to the microgrid according to Fig. 9. Fig. 10 depicts the frequency response of the microgrid in terms of disturbances. The maximum frequency deviation using the proposed method is 0.13 Hz. The maximum frequency deviation using the multi-objective fuzzy proportional-integral controller type 2 optimized by the black hole algorithm is 0.97 Hz. The maximum frequency deviation using the multi-objective proportional-integral controller optimized with the black hole algorithm is 0.73 Hz. As can be seen in the simulation results, the proposed RMPC controller in comparison with the multi-objective proportional-integral controller optimized with a black hole algorithm [28] and multi-objective fuzzy-proportional integral controller type 2 optimized with the black hole algorithm [28] has a better response speed and lower fluctuation and is more robust to distributed energy resources disturbances.

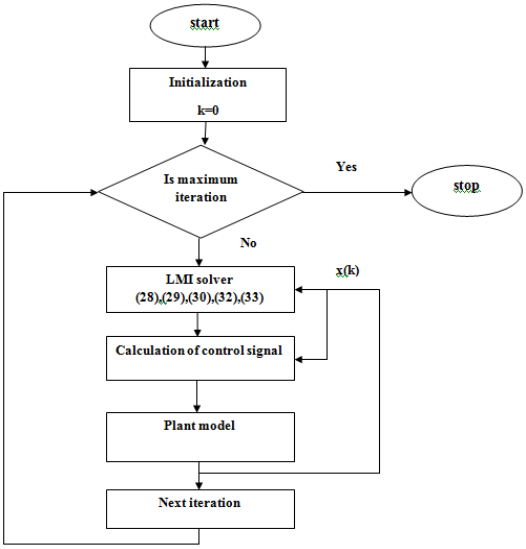

Fig. 6: The flowchart of the proposed method.

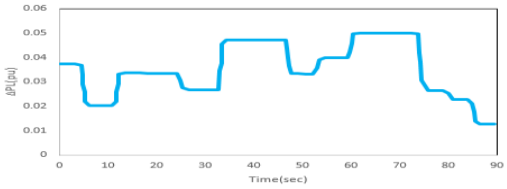

Fig. 7: The load disturbances.

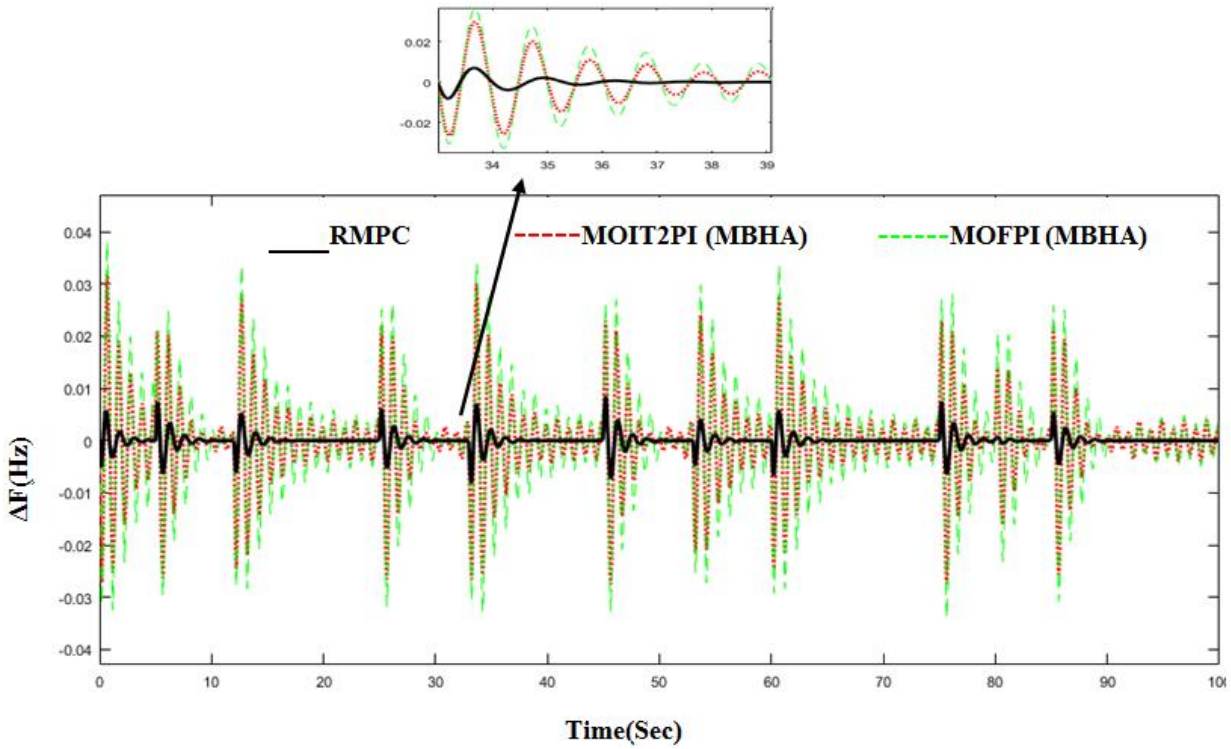

Fig. 8: The frequency response of the microgrid.

Table 1: The parameters of the microgrid on the shipboard.

Parameter	Value	Parameter	Value
T_g	2s	T_{fess}	0.1s
T_d	1s	T_{bess}	0.1s
R	3(pu Mw/second)	T_c	0.5s
T_G	0.5s	T_{pv}	4s
T_h	4s	C_p	0.195
D	0.012(pu/Hz)	ρ_A	1.225Km/m^3
T(mpc)	0.1		

Scenario (3): In this scenario, changes in distributed energy resources are not considered and only load disturbances are considered with the uncertainty in parameters. Table 2 shows the changes in the parameters related to the microgrid. The load disturbances have been applied to the microgrid according to Fig. 7, taking into account the uncertainty of the parameters. The frequency response of the microgrid in terms of load disturbances is depicted in Fig. 11. The maximum frequency deviation using the proposed method is 0.006 Hz. The maximum frequency deviation using the multi-objective fuzzy proportional-integral controller type 2 optimized by the black hole algorithm is 0.034 Hz. The maximum frequency deviation using the multi-objective proportional-integral controller optimized with the black hole algorithm is 0.042 Hz. As can be seen in the simulation results, the proposed RMPC controller in comparison with the multi-objective proportional-integral controller optimized with the black hole algorithm [28] and multi-objective fuzzy-proportional-integral controller type 2 optimized with the black hole algorithm [28] has a better response speed and lower fluctuation and is more robust to parameter uncertainties.

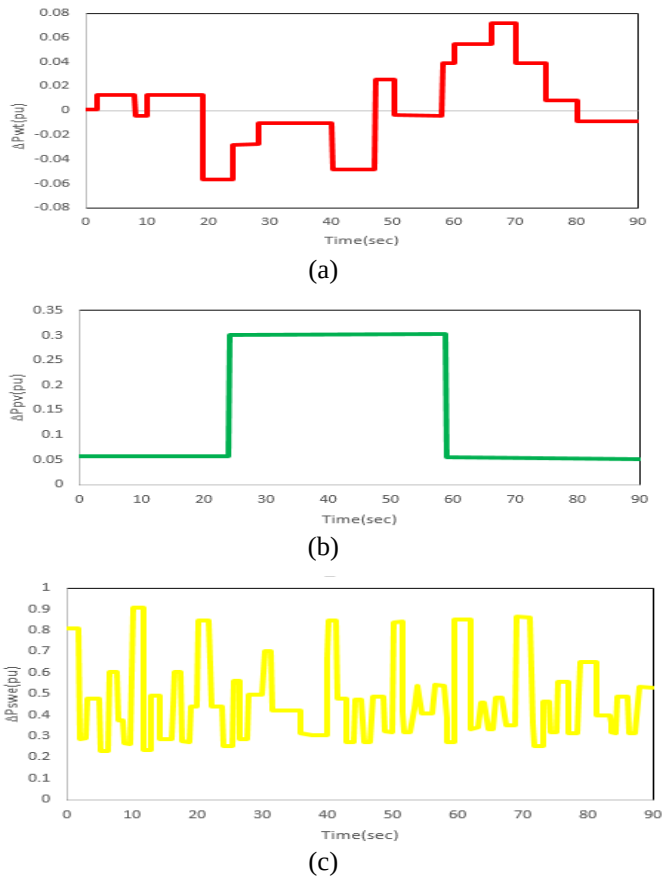

Fig. 9: Disturbances of (a) the wind turbine, (b) photovoltaic, and (c) sea wave.

Scenario (4): In this scenario, changes in distributed energy resources and load disturbances are considered. Fig. 12 shows the changes in distributed generation sources.

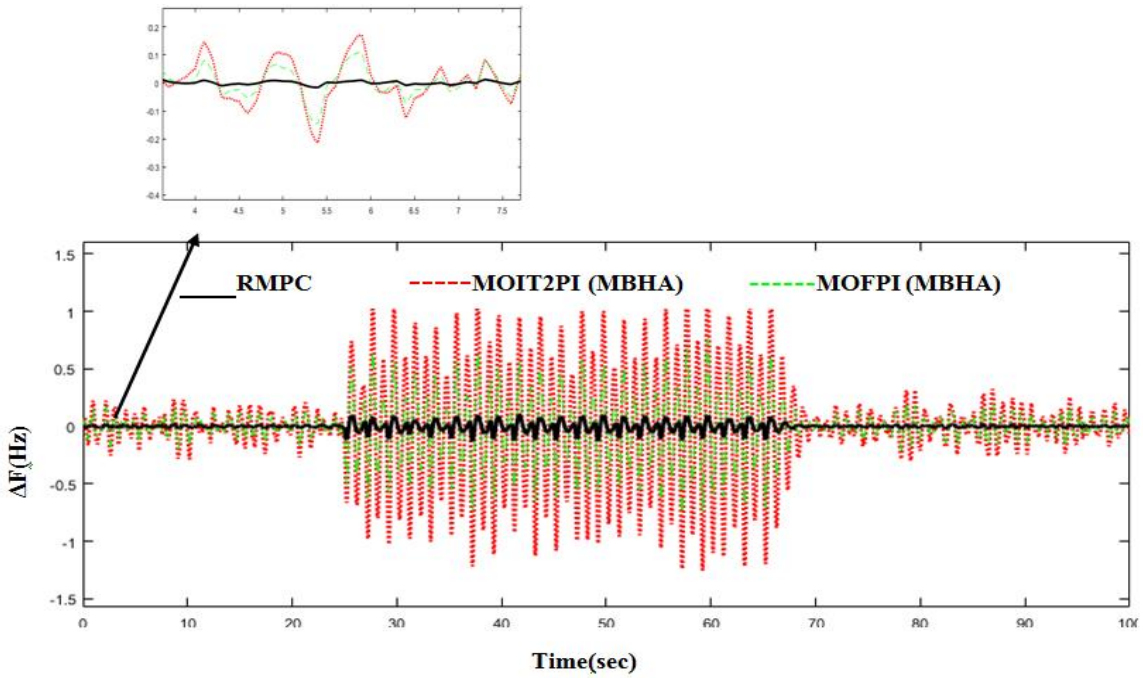

Fig. 10: The frequency response of the microgrid.

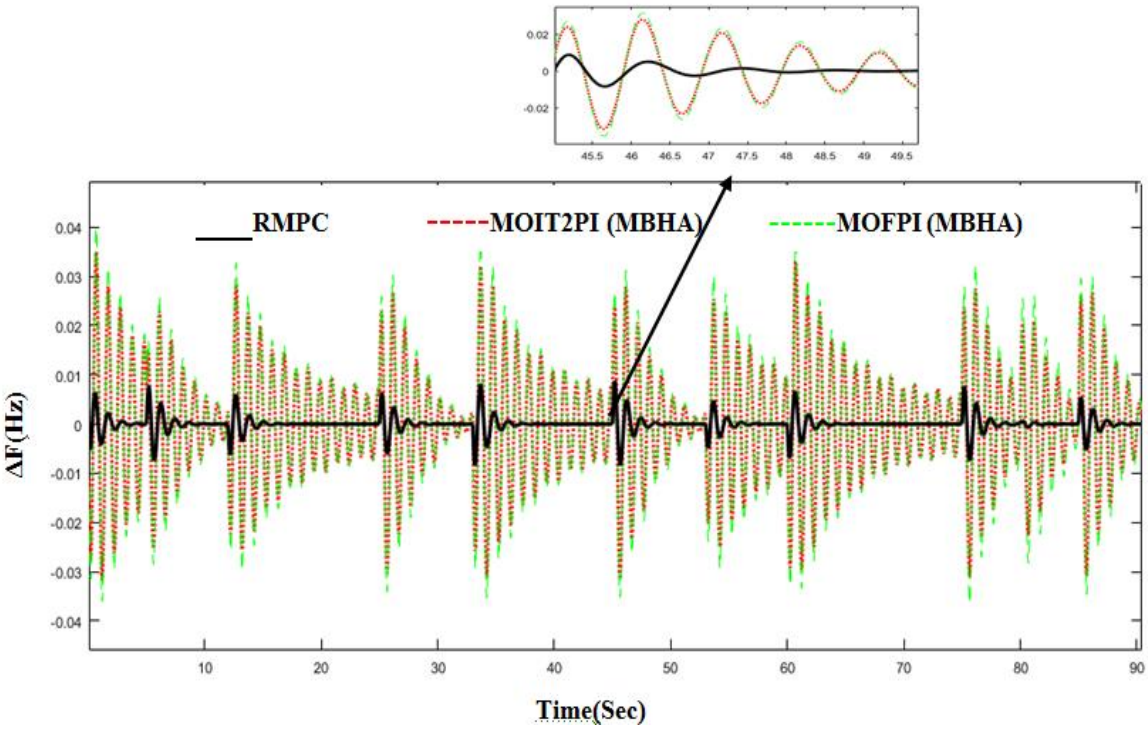

Fig. 11: The frequency response of the microgrid.

Table 2: The changes in the microgrid parameters.

Parameter	Range
R	+25%
D	-15%
M	+45%
T_e	-35%
T_g	+15%
T_{fess}	-15%
T_{bess}	+25%

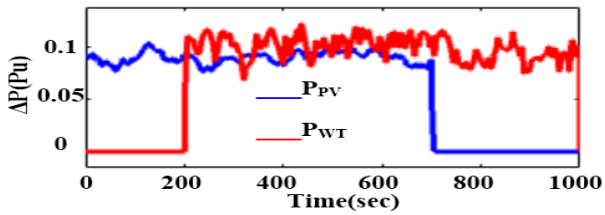

Fig. 12: The changes in distributed generation sources.

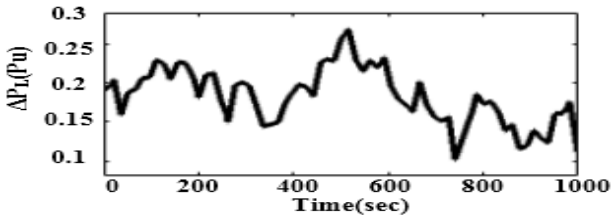

Fig. 13: Load changes applied to the islanded microgrid.

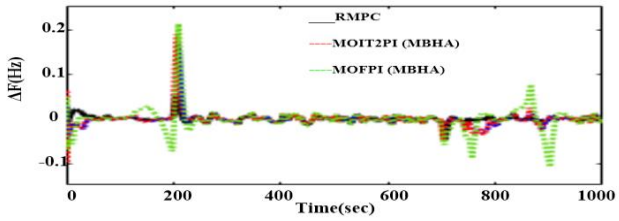

Fig. 14: The frequency response of the microgrid.

Fig. 13 shows the load changes applied to the islanded microgrid. Fig. 14 shows the microgrid frequency response to changes in distributed generation and load sources. The maximum frequency deviation using the proposed method is 0.05 Hz. The maximum frequency deviation using the multi-objective fuzzy proportional-integral controller type 2 optimized by the black hole algorithm is 0.17 Hz. The maximum frequency deviation using the multi-objective proportional-integral controller optimized with the black hole algorithm is 0.21 Hz.

5. Conclusion

The issue of frequency stability in microgrids is important. One of the most important components for improving frequency stability is the load-frequency control loop. The load-frequency control loop is used to improve the microgrid frequency stability and return the frequency to the nominal value after a fault. In this paper, a control method (predictive controller of a robust model based on linear matrix inequality) is designed in the load-frequency control structure. According to the results, the frequency fluctuations due to load disturbances have been reduced by 80% using the proposed method (compared to other methods proposed in this field). Frequency fluctuations caused by load disturbances and uncertainty of system parameters have been reduced by 82% using the proposed method compared to the other methods proposed in this field. Frequency fluctuations induced by disturbances of distributed energy resources have been reduced by 82% using the proposed method versus the other methods proposed in this field. According to these results, the proposed method is very robust to disturbances and uncertainty of microgrid parameters and improves the microgrid frequency stability on the shipboard.

Credit Authorship Contribution Statement

Farhad Amiri: Conceptualization, Data curation, Formal analysis, Methodology, Resources, Software, Roles/Writing - original draft, Writing - review & editing. **Mohammad Hassan Moradi:** Supervision, Validation.

Declaration Of Competing Interest

The authors declare that they have no known competing financial interests or personal relationships that could have appeared to influence the work reported in this paper. The ethical issues, including plagiarism, informed consent, misconduct, data fabrication and/or falsification, double publication and/or submission, and redundancy, have been completely observed by the authors.

References

[1] F. Amiri, and A. Hatami, "A model predictive control method for load-frequency control in islanded microgrids," *Computational Intelligence in Electrical Engineering*, vol. 8, no. 1, pp. 9-24, 2017.

[2] F. Amiri, and M. H. Moradi, "Coordinated control of LFC and SMES in the power system using a new robust controller," *Iranian Journal of Electrical and Electronic Engineering*, vol. 17, no. 4, pp. 1912-1912, 2021.

[3] F. Amiri, and M. H. Moradi, "Designing a fractional frder PID controller for a two-area micro-grid under uncertainty of parameters," *Iranian Journal of Energy*, vol. 20, no. 4, pp. 49-78, 2018.

[4] F. Amiri, and A. Hatami, "Nonlinear Load frequency control of isolated microgrid using fractional order PID based on hybrid craziness-based particle swarm optimization and pattern search," *Journal of Iranian Association of Electrical and Electronics Engineers*, vol. 17, no. 2, pp. 135-148, 2020.

[5] D. K. Lal, A. K. Barisal, and M. Tripathy, "Load frequency control of multi area interconnected microgrid power system using grasshopper optimization algorithm optimized fuzzy PID controller," in *2018 Recent Advances on Engineering, Technology and Computational Sciences (RAETCS)*, 2018, pp. 1-6.

[6] Y. Yang, C. Li, J. Xu, F. Blaabjerg, and T. Dragičević, "Virtual inertia control strategy for improving damping performance of DC microgrid with negative feedback effect," in *IEEE Journal of Emerging and Selected Topics in Power Electronics*, vol. 9, no. 2, pp. 1241-1257, April 2021.

[7] F. Amiri, and M. H. Moradi, "A new control strategy for controlling isolated microgrid," *The Journal of Energy: Engineering & Management*, vol. 10, no. 4, pp. 60-73, 2021.

[8] D. C. Das, A. Roy, and N. Sinha, "GA based frequency controller for solar thermal diesel-wind hybrid energy generation/energy storage system," *International Journal of Electrical Power & Energy Systems*, vol. 43, no. 1, pp. 262–79, 2012.

[9] D. C. Das, A. K. Roy, and N. Sinha, "PSO based frequency controller for wind-solar-diesel hybrid energy generation/energy storage system," in *2011 International Conference on Energy, Automation and Signal*, Bhubaneswar, Odisha, 2011, pp. 1-6.

[10] R. H. Kumar, and S. Ushakumari, "Biogeography-based Tuning of PID controllers for load frequency

control in microgrid," in *2014 International Conference on Circuit, Power and Computing Technologies [ICCPCT], Nagercoil*, 2014, pp. 797-802.

[11] G. Shankar, and V. Mukherjee, "Load frequency control of an autonomous hybrid power system by quasi-oppositional harmony search algorithm," *International Journal of Electrical Power & Energy Systems*, vol. 78, pp. 715–734, 2016.

[12] M. Shahbazi, and F. Amiri, "Designing a neuro-fuzzy controller with CRPSO and RLSE algorithms to control voltage and frequency in an isolated microgrid," *2019 International Power System Conference (PSC)*, 2019, pp. 588-594.

[13] I. Pan, and S. Das, "Fractional order fuzzy control of hybrid power system with renewable generation using chaotic PSO," *The International Society of Automation*, vol. 62, pp. 19-29, 2016.

[14] M. H. Khooban, T. Niknam, F. Blaabjerg, P. Davari, and T. Dragicevic, "A robust adaptive load frequency control for micro-grids," *The International Society of Automation*, vol. 65, pp. 220-229, 2016.

[15] M.H. Khooban, T. Niknam, F. Blaabjerg, P. Davari, and T. Dragicevic, "A new load frequency control strategy for micro-grids with considering electrical vehicles," *Electric Power Systems Research*, vol. 143, pp. 585-598, 2017.

[16] V. P. Singh, S. R. Mohanty, N. Kishor, and P. K. Ray, "Robust H-infinity load frequency control in hybrid distributed generation system," *International Journal of Electrical Power & Energy Systems*, vol. 46, pp. 294-305, 2013.

[17] H. Bevrani, M. R. Feizi, and S. Ataee, "Robust frequency control in an islanded microgrid: H-infinity and μ-synthesis approaches," *IEEE Transactions on Smart Grid*, vol. 7, no. 2, pp. 706-717, March 2016.

[18] S. M. Azizi, and S. A. Khajehoddin, "Robust load frequency control in islanded microgrid systems using μ-synthesis and D-K iteration,"*2016 Annual IEEE Systems Conference (SysCon)*, Orlando, 2016, pp. 1-8.

[19] H. Bevrani, F. Habibi, P. Babahajyani, M. Watanabe, and Y. Mitani, "Intelligent frequency control in an ac microgrid: online pso-based fuzzy tuning approach," *IEEE Transactions on Smart Grid*, vol. 3, no. 4, pp. 1935-1944, 2012.

[20] M. Khalghani, M. Khooban, M. Moghaddam, N. Vafamand, and M. Goodarzi, "A self-tuning load frequency control strategy for microgrids: Human brain emotional learning," *International Journal of Electrical Power & Energy Systems*, vol. 75, pp. 311-319, 2016.

[21] V. P. Singh, N. Kishor, and S. Paulson, "Communication time delay estimation for load frequency control in two-area power system," *Ad Hoc Networks*, vol. 41, pp. 69-85, 2016.

[22] F. Tedesco, and A. Casavola, "Fault-tolerant distributed load/frequency coordination strategies for multi-area power microgrids," *International Federation of Automatic Control –Papers OnLine*, vol. 48, no. 21, pp. 54-59, 2015.

[23] R. Fan, J. Zhao, B. Pan, N. Chen, T. Wang, and H. Ma,"Automatic generation control of three-area small hydro system based on fuzzy PID control," in *2014 International Conference on Power System Technology*, Chengdu, 2014, pp. 2522-2528.

[24] P. Ray, S. Mohanty, and N. Kishor,"2010. Small-signal analysis of autonomous hybrid distributed generation systems in presence of ultracapacitor and tie-line operation," *Journal of Electrical Engineering*, vol. 61, no. 4, pp. 205-214, 2010.

[25] G. Messinis *et al.*, "A multi-microgrid laboratory infrastructure for smart grid applications," *MedPower 2014*, Athens, 2014. pp. 1-6.

[26] D. I. Makrygiorgou and A. T. Alexandridis, "Nonlinear modeling, control and stability analysis of a hybrid ac/dc distributed generation system," in *2017 25th Mediterranean Conference on Control and Automation (MED)*, 2017, pp. 768-773.

[27] H. M. Hasanien, and A. A. El-Fergany, "Salp swarm algorithm-based optimal load frequency control of hybrid renewable power systems with communication delay and excitation cross-coupling effect," *Electric Power Systems Research*, vol. *176*, 105938, 2019.

[28] M. H. Khooban, T. Dragicevic, F. Blaabjerg, and M. Delimar, "Shipboard microgrids: A novel approach to load frequency control," *IEEE Transactions on Sustainable Energy*, vol. 9, no. 2, pp. 843-852, 2018.

[29] G. Magdy, G. Shabib, A. A. Elbaset, and Y. Mitani, "Renewable power systems dynamic security using a new coordination of frequency control strategy based on virtual synchronous generator and digital frequency protection," *International Journal of Electrical Power & Energy Systems*, vol. *109*, pp. 351-368, 2019.

[30] F. Amiri, and M. Moradi, "Microgrid on the ship: load Frequency- control of the microgrid, taking into account the Sea Wave energy by the optimized model predictive controller," *Journal of Renewable and New Energy*, vol. 8, no. 1, pp. 78-90, 2021.

[31] F. Amiri, and M. Moradi, "Designing a new robust control for virtual inertia control in the microgrid with regard to virtual damping," *Journal of Electrical and Computer Engineering Innovations (JECEI)*, vol. 8, no. 1, pp. 53-70, 2020.

[32] M. H. Moradi, and F. Amiri, "Virtual inertia control in islanded microgrid by using robust model predictive control (RMPC) with considering the time delay," *Soft Computing*, vol. 25, no. 8, pp. 6653-6663, 2021.

[33] F. Amiri, and M. H. Moradi, "Angular speed control in a hybrid stepper motor using linear matrix inequality," *Computational Intelligence in Electrical Engineering*, vol. 12, no. 3, pp. 33-50, 2020.

[34] F. Amiri, and M. H. Moradi, "Designing a new robust control method for AC servo motor," *Journal of Nonlinear Systems in Electrical Engineering*, vol. 7, no. 1 pp. 55-80, 2020.

[35] M. H. Moradi, and F. Amiri, "Load frequency control in a two area microgrid by optimized model predictive controller," *Journal of Iranian Association of Electrical and Electronics Engineers*, vol. 19, no. 1, 2021.

[36] F. Amiri, and S. Afshar, "Load frequency control via adaptive fuzzy PID sontroller in an isolated microgrid,"in *2017 International Power System Conference (PSC).* 2017.

BIOGRAPHY

Farhad Amiri was born in Ilam, Iran. He received his M.Sc. degree in Electrical Engineering from Bu-Ali Sina University in 2017. He is currently working toward his Ph.D. degree in Electrical Engineering at Bu-Ali Sina University**.** His research interests include dynamic and transient operation of power systems, control, microgrids, and renewable energy.

Mohammad Hassan Moradi was born in Nowshahr, Mazandaran, Iran. He obtained his B.Sc., M.Sc. and Ph.D. from the Sharif University of Technology, Tarbiat Modares University, and Strathclyde University in Glasgow, Scotland in 1991 1993, and 2002, respectively. His research interests include new and green energy, microgrid modeling and control, DG location and sizing in power systems, photovoltaic systems and power electronics, combined heat and power plant, power quality, supervisory control, and fuzzy control.